ChemComm

Cite this: *Chem. Commun.*, 2011, **47**, 8400–8402

www.rsc.org/chemcomm

COMMUNICATION

Heteroepitaxial growth of ZnO branches selectively on TiO_2 nanorod tips with improved light harvesting performance†

Feng Gu,[ab] Lili Gai,[a] Wei Shao,[a] Chunzhong Li*[a] and Lukas Schmidt-Mende*[b]

Received 20th April 2011, Accepted 8th June 2011
DOI: 10.1039/c1cc12309b

A seeded heteroepitaxial growth of ZnO nanorods selectively on TiO_2 nanorod tips was achieved by restricting crystal growth on highly hydrophobic TiO_2 nanorod film surfaces. Intriguing light harvesting performance and efficient charge transport efficiency has been found, which suggest potential applications in photovoltaics and optoelectronics.

Recently, branched nanowires (NWs) have attracted much interest due to their special tree-like structures offering greatly enhanced surface area and a direct conduction pathway for the rapid collection of photogenerated electrons,[1] and therefore promise very attractive potential applications in optoelectronics, photocatalysis, photovoltaics and sensing.[1d,2] One of the key remaining issues in the field is the development of single-crystal nanobranches with an epitaxial relation to the trunk to diminish the possibility of charge recombination during interparticle percolation.[3] Although there have been a few reports on the formation of branched NWs with different inorganic components fused together,[2b,4] these systems impose interfaces between materials with large lattice mismatch, with the formation of a large quantity of defects at grain boundaries as trapping sites, adversely affecting charge migration.[5]

ZnO and TiO_2 are the most investigated semiconductor materials for optoelectronic applications. ZnO is a direct band gap semiconductor with a wide band gap (E_g = 3.37 eV) and large binding energy, high electrical conductivity and transparency in the visible region. After coupling with TiO_2 to form a ZnO–TiO_2 heterostructure, faster electron transport with reduced recombination loss can be expected because the electron mobility of ZnO is higher by 2–3 orders of magnitude than that of TiO_2.[1c,6] In this communication, a heteroepitaxial growth of ZnO nanorods selectively on the tips of TiO_2 nanorods to form special dandelion-like heterostructures was achieved by restricting the seed planting and the following crystal growth on the film surface, based on the highly hydrophobic property of the TiO_2 nanorod film. Selective growth of metal or semiconductor dots on the secondary structure is of particular importance because of the strong coupling of electronic states and unusual properties.[7] This strategy is an effective and simple attempt for the selective growth of nanostructures with controlled density and location on the secondary component by taking advantage of the macroscopic wettability of materials. Arising from this special branched structure with heteroepitaxial interfaces, intriguing light harvesting performance and better electron transport efficiencies are exhibited, which imply potential applications in the fields of photovoltaics and optoelectronics.

A key step enabling our design is to realize the selective deposition of a seed layer on the nanorod tips and prevent the precursor solution penetrating the grooves during the following crystal growth process. A hydrothermally derived rutile TiO_2 nanorod film[8] with rod length of ~1.3 μm and diameter of ~90 nm is shown in Fig. 1a and b. The wettability was evaluated by water contact angel (CA) measurement of the as-prepared film. Fig. 1c shows a spherical water droplet with a water CA of 131.3°, indicating a highly hydrophobic surface of the rutile TiO_2 nanorod film. Although rutile TiO_2 is a hydrophilic material with a water CA of 74° on a smooth single crystal (001) surface,[9] highly hydrophobic, even super-hydrophobic surfaces of TiO_2 can be achieved in the case of special geometrical morphology of the film surface.[10] Therefore, when wetting the film with zinc acetate solution, the solution would not penetrate the grooves and is suspended on the surface of the nanorod films as droplets. After the decomposition

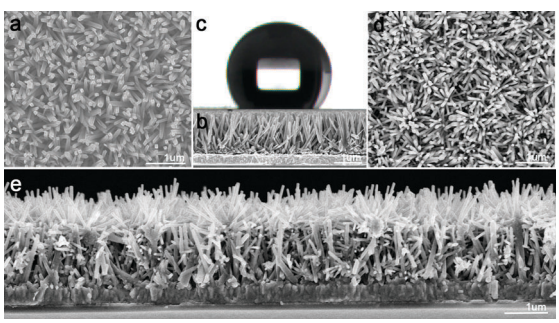

Fig. 1 (a, b) SEM images of rutile TiO_2 nanorod film. (c) Photograph of a water droplet on the TiO_2 nanorod film. (d, e) SEM images of the ZnO/TiO_2 branched heterostructures.

[a] *Key Laboratory for Ultrafine Materials of Ministry of Education, School of Materials Science and Engineering, East China University of Science & Technology, Shanghai 200237, China. E-mail: czli@ecust.edu.cn; Fax: 86-21- 6425-0624; Tel: 86-21-6425-0949*
[b] *Department of Physics and Center for NanoScience (CeNS), Ludwig-Maximilians University (LMU), Munich80799, Germany. E-mail: L.Schmidt-Mende@physik.uni-muenchen.de; Fax: 49-89-2180-17836; Tel: 49-89-2180-3443*
† Electronic supplementary information (ESI) available. See DOI: 10.1039/c1cc12309b

procedure, textured ZnO nanocrystals were stacked on the platforms supplied by the TiO_2 tips without slumping into the grooves. Hydrothermal growth of ZnO nanorods on the seeded substrate was conducted according to the technique reported previously.[11] Fig. 1d and e show the scanning electron microscopy (SEM) images of the obtained heterogeneous nanostructures (HNs). Dense hexagonal ZnO nanorods with diameter of 50 nm and length of 1000 nm grow divergently on the TiO_2 nanorod tips and form 3D branched NW heterostructures. ZnO nanorod bundles were only decorated on the TiO_2 nanorod tips with naked side surfaces, implying the selective anisotropic crystal growth on TiO_2 nanorods. Large corollas covering the entire TiO_2 nanorod film surface, by interweaving with neighbours, allow the incident light to be strongly scattered and to improve the light harvesting efficiency.

The crystallographic relationship between the TiO_2 trunk and ZnO branch has been further analyzed by high-resolution transmission electron microscopy (HRTEM) measurements. Fig. 2a shows a HRTEM image taken at the junction of TiO_2 and ZnO, while insets of this figure are SAED patterns recorded by focusing specifically at the TiO_2 and ZnO regions, respectively. ZnO nanorods grew on the TiO_2 rod tip along the 002 *c*-direction with a lattice spacing of 0.26 nm and a clean interface can be observed clearly. Examination of the TiO_2 indicates that the single-crystalline TiO_2 nanorods are of a rutile phase with growth along the [001] direction as evidenced by the SAED pattern examined along the $[1\bar{1}0]$ zone axis. Lattice fringes with interplanar spacings, $d_{110} = 0.32$ nm and $d_{001} = 0.29$ nm, are clearly imaged. The HRTEM result reveals that the ZnO nanorod is not growing perpendicular to the TiO_2 nanorod surface but with an angle of 27°, presumably because the ZnO (002) crystal planes ($d_{002} = 0.26$ nm) would gear at an angle to match the TiO_2 (001) crystal planes ($d_{001} = 0.29$ nm) largely to relax strain ($d_{ZnO(002)} = d_{TiO_2(001)}\cos\theta$, $\theta = 27°$), confirming the epitaxial correlation for these HNs. A lattice-fringe-resolved HRTEM image is also shown in Fig. 2b, evidencing the crystallographic (002) planes of ZnO intercalated TiO_2 (001) planes with an angle of 27°. A 2D atomic arrangement with a twisted angle of 27° shown in Fig. S1† further demonstrates the epitaxial relationship between the TiO_2 nanorod and ZnO branches by considering the observed (001)/(002) interface with zone axes of $[1\bar{1}0]$ and [010] for TiO_2 and ZnO, respectively.

The ZnO seeds, with a heteroepitaxial interface from which the heterogeneous nucleation takes place preferentially to form well-defined ZnO branches, is the essence to obtain the final interesting HNs. The lattice mismatch between the {001} planes of rutile TiO_2 and the {002} planes of wurtzite ZnO is small, noting that the interplanar distances of d_{001} (0.29 nm, TiO_2) and d_{002} (0.26 nm, ZnO) is similar, which might present a heteroepitaxial characteristic at the interface by simple modulation of the lattices with a small angle to largely release the strain. ZnO seeds deposited on TiO_2 tip with multiple lattice orientations and then the deposited ZnO extended to neutralize local polar charge and release the strain accumulated. By serving as starting positions, the epitaxial growth of ZnO took place. Considering the strain induced at the interface, only minor strain can be detected, further confirming the largely strain free relaxation due to congruent lattice fringes (Fig. S2†). Furthermore, the ZnO nanorods were found to anchor to TiO_2 nanorod tips with point contacts induced by the seeds (Fig. S3†). The HRTEM image shown in Fig. S4† evidenced the formation of ZnO seeds anchoring to the TiO_2 nanorod outer surface with lattice modulation, presumably induced by the strain from the lattice mismatch. Generally, a key step in obtaining single-crystal epitaxy is to remove the native oxide layer to generate a clean interface between the deposited amorphous material in a pore and the c-Si substrate.[3] For Si NW-based epitaxial growth, if the native oxide was not removed completely, the crystal orientation in the film was independent of the substrate orientation.[3] It is also reported that ZnO seeds failed to lead to a coating on a Si nanowire surface after removing native oxide.[12] However, in our work, the decomposition of zinc salts was effective to deposit ZnO seeds onto the TiO_2 nanorod tips without any further surface modification process to the TiO_2 film. Top and side views in Fig. 1a and b show that the top surface of the TiO_2 nanorods appears to contain many step edges, while the side surface is smooth, as the crystal growth of rutile TiO_2 nanorods proceeds *via* ledge growth mechanism by addition of titanium growth units (*e.g.*, $[Ti(OH)_2Cl_2(OH)_2]^0$) at the step edges.[13] The step edges may allow for more seeds formed with diverse directions and as a result dandelion-like ZnO/TiO_2 HNs were formed (Fig. 1d). Upon addition of polyethylenimine (PEI) as a retardant, ZnO nanorods with similar diameters were obtained. PEI was adapted to affect the growth habit of ZnO nanorods by adsorption on the nonpolar facets of ZnO crystal and by coordination to zinc ions.[14] In this work, by changing parameters such as addition of PEI or hexamethylenetetramine (HMT), or reaction time, ZnO nanorods with different lengths of 200–1000 nm branched out on the TiO_2 tip (Fig. S5†), which can interweave with neighbouring counterparts to form a complex and dense canopy, implying an excellent light scattering capability. Synthetic process and typical morphologies of the HNs were given in the ESI†.

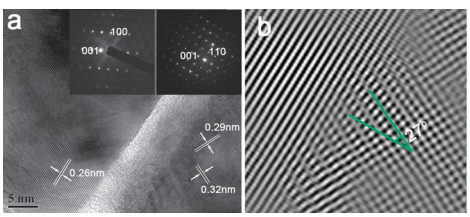

Fig. 2 (a) HRTEM image at the interface with corresponding SAED patterns of the two components. (b) Lattice-fringe-resolved HRTEM image showing the lattice spacings at the interface.

Photoluminescence (PL) was used to study the structure and defects of the ZnO/TiO_2 NHs (Fig. 3). The HN films show a strong emission peak at ~378 nm (UV emission) due to the excitonic transition of ZnO[15] with a weak broad emisson at ~394 nm arising from the lowest indirect transition (X1 → Γ1) of rutile TiO_2.[16] It should be noted that the known "green" emission cannot be detected in the range of 420–600 nm, indicating very low residual defects in the structures, due to high crystallinity of the HNs, even after heteroepitaxial growth of ZnO rods. Increasing the ZnO rod length would result in the PL intensity enhancement of the two components, not only the excitonic emission from ZnO but also that from

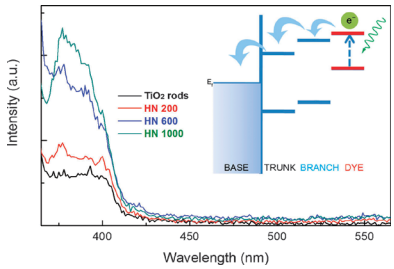

Fig. 3 Photoluminescent spectra of ZnO/TiO_2 HN films and TiO_2 nanorod film.

rutile TiO_2, indicating an efficient electron transfer occurs upon excitation.

Compared with the PL spectrum of ZnO nanorod film with similar length (Fig. S6†), the excitonic emission from ZnO weakened while the emission from TiO_2 was improved after forming the HNs, further proving the charge transfer behavior. ZnO has higher electron mobility (100–205 $cm^2\ V^{-1}\ s^{-1}$) and carrier concentration ($\sim$1018 cm^{-3}) than rutile TiO_2.[1c,6] Therefore, due to the congruent interface and axial surface field within each nanorod, much more electrons photogenerated in ZnO may swarm into the TiO_2 rod with reduced recombination loss (usually by residual defects located at the interface) and as a result the PL intensity from rutile TiO_2 increased greatly. The efficient electron transfer and collection efficiencies enable the HNs to find possible uses in areas such as energy generation and storage.

Light scattering properties were studied by measuring the diffuse reflection spectra (Fig. S7†). Compared with TiO_2 nanorod film, the measured reflectance of ZnO/TiO_2 HNs (branch lengths of 600, 1000 nm) was found to be remarkably higher than that of TiO_2 nanorods, indicating a superior light scattering effect. With increasing the length of ZnO branches, better reflection can be obtained due to the interwoven corollas constructed by ZnO nanorods, which can effectively confine the incident light within the film. Assuming the corollas as quasi-spheres, such scattering trend was found to be similar to the results estimated from Mie resonance theory;[17] as the size of the corolla is comparable with the wavelength of the incident light, resonant scattering most likely occurs. The corolla was constructed by branched ZnO nanorods and further interwoven with the neighboring counterparts to form a dense scattering layer, such special structure can generate multiple scattering to light and the formation of closed loops for light confinement,[18] and as a result, to increased light harvesting efficiency, especially when coupling with dyes and quantum dots in photovoltaic cells (inset of Fig. 3). The on-going research is focusing on the photovoltaic properties of the HNs.

In summary, we have reported a simple and effective solution approach for the selective growth of ZnO nanorods onto tip-seeded TiO_2 nanorod arrays to form special dandelion-like ZnO/TiO_2 heterogeneous nanostructures by exploiting the high hydrophobicity characteristics of TiO_2 nanorod film. The branched ZnO nanorods were found to possess a strain-induced epitaxial relation to the TiO_2 trunk, and thereby prominent charge transport, along with light harvesting efficiencies were exhibited. This strategy is a new concept for position-selective growth of homo- or heterostructured nanomaterials, which is certainly significant for future optoelectronic applications.

This work was supported by the National Natural Science Foundation of China (20925621, 81071994), Shanghai Rising-Star Program (09QH1400700), Program of Shanghai Subject Chief Scientist (09XD1400800), Basic Research Program of Shanghai (10JC1403300) and Alexander von Humboldt Foundation.

Notes and references

1 (*a*) D. L. Wang and C. M. Lieber, *Nat. Mater.*, 2003, **2**, 355; (*b*) J. Zhu, H. L. Peng, A. F. Marshall, D. M. Barnett, W. D. Nix and Y. Cui, *Nat. Nanotechnol.*, 2008, **3**, 477; (*c*) S. H. Ko, D. Lee, H. W. Kang, K. H. Nam, J. Y. Yeo, S. J. Hong, C. P. Grigoropoulos and H. J. Sung, *Nano Lett.*, 2011, **11**, 666; (*d*) K. Sun, Y. Jing, N. Park, C. Li, Y. Bando and D. L. Wang, *J. Am. Chem. Soc.*, 2010, **132**, 15465.
2 (*a*) J. Y. Lao, J. G. Wen and Z. F. Ren, *Nano Lett.*, 2002, **2**, 1287; (*b*) S. Y. Bae, H. W. Seo, H. C. Choi and J. Park, *J. Phys. Chem. B*, 2004, **108**, 12318.
3 H. Arora, P. Du, K. W. Tan, J. K. Hyun, J. Grazul, H. L. Xin, D. A. Muller, M. O. Thompson and U. Wiesner, *Science*, 2010, **330**, 214.
4 (*a*) Y. Lei, G. Zhao, M. Liu, Z. Zhang, X. Tong and T. Cao, *J. Phys. Chem. C*, 2009, **113**, 19067; (*b*) Y. K. A. Lau, D. J. Chernak, M. J. Bierman and S. Jin, *J. Mater. Chem.*, 2009, **19**, 934.
5 K. W. Kwon and M. Shim, *J. Am. Chem. Soc.*, 2005, **127**, 10269.
6 D. C. Look, D. C. Reynolds, J. R. Sizelove, R. L. Jones, C. W. Litton, G. Cantwell and W. C. Harsch, *Solid State Commun.*, 1998, **105**, 399.
7 (*a*) X. H. Li, J. Lian, M. Lin and Y. Chan, *J. Am. Chem. Soc.*, 2011, **133**, 672; (*b*) W. S. Wang, J. Goebl, L. He, S. Aloni, Y. X. Hu, L. Zhen and Y. D. Yin, *J. Am. Chem. Soc.*, 2010, **132**, 17316; (*c*) R. D. Robinson, B. Sadtler, D. O. Demchenko, C. K. Erdonmez, L. W. Wang and A. P. Alivisatos, *Science*, 2007, **317**, 355; (*d*) T. Mokari, E. Rothenberg, I. Popov, R. Costi and U. Banin, *Science*, 2004, **304**, 1787.
8 B. Liu and E. S. Aydil, *J. Am. Chem. Soc.*, 2009, **131**, 3985.
9 (*a*) X. J. Feng, J. Zhai and L. Jiang, *Angew. Chem., Int. Ed.*, 2005, **44**, 5115; (*b*) R. Wang, N. Sakai, A. Fujishima, T. Watanabe and K. Hashimoto, *J. Phys. Chem. B*, 1999, **103**, 2188.
10 (*a*) S. Minko, M. Muller, M. Motornov, M. Nitschke, K. Grundke and M. Stamm, *J. Am. Chem. Soc.*, 2003, **125**, 3896; (*b*) X. J. Feng, L. Feng, M. H. Jin, J. Zhai, L. Jiang and D. B. Zhu, *J. Am. Chem. Soc.*, 2004, **126**, 62.
11 L. E. Greene, M. Law, D. H. Tan, M. Montano, J. Goldberger, G. Somorjai and P. Yang, *Nano Lett.*, 2005, **5**, 1231.
12 D. Mudusu, K. R. Nandanapalli, P. Alexander and P. Fernando, *ChemPhysChem*, 2010, **11**, 809.
13 A. Pottier, C. Chaneac, E. Tronc, L. Mazerolles and J. P. Jolivet, *J. Mater. Chem.*, 2001, **11**, 1116.
14 L. E. Greene, B. D. Yuhas, M. Law, D. Zitoun and P. D. Yang, *Inorg. Chem.*, 2006, **45**, 7535.
15 G. Adamopoulos, A. Bashir, S. Thomas, W. P. Gillin, S. Georgakopoulos, M. Shkunov, M. A. Baklar, N. Stingelin, R. C. Maher, L. F. Cohen, D. D. C. Bradley and T. D. Anthopoulos, *Adv. Mater.*, 2010, **22**, 4764.
16 F. X. Liu, M. Tang, L. Liu, S. Lu, J. Y. Wang, Z. Y. Chen and R. Ji, *Phys. Status Solidi A*, 2000, **179**, 437.
17 (*a*) Q. F. Zhang, T. P. Chou, B. Russo, S. A. Jenekhe and G. Cao, *Adv. Funct. Mater.*, 2008, **18**, 1654; (*b*) S. M. Scholz, R. Vacassy, J. Dutta, H. Hofmann and M. Akinc, *J. Appl. Phys.*, 1998, **83**, 7860.
18 (*a*) D. S. Wiersma, P. Bartolini, A. Lagendijk and R. Righini, *Nature*, 1997, **390**, 671; (*b*) H. Cao, J. Y. Xu, D. Z. Zhang, S. H. Chang, S. T. Ho, E. W. Seelig, X. Liu and R. P. H. Chang, *Phys. Rev. Lett.*, 2000, **84**, 5584.